Is whole body low dose CT still necessary in the era of ^{18}F-FDG PET/CT for the assessment of bone disease in multiple myeloma patients?

Nicola Maggialetti[1] MD,
Cristina Ferrari[2] MD,
Anna Giulia Nappi[2] MD,
Angela Quinto[3] MD,
Bernardo Rossini[3] MD,
Marcello Zappia[1] MD,
Carla Minoia[3] MD,
Attilio Guarini[3] MD,
Luca Brunese[1] MD,
Giuseppe Rubini[2] MD

1. Department of Medicine and Health Sciences "V. Tiberio", University of Molise, Campobasso, Italy,
2. Interdisciplinary Department of Medicine, Nuclear Medicine Unit, University of Bari Aldo Moro, Piazza Giulio Cesare 11 - 70124 Bari, Italy,
3. Hematology Unit- IRCCS Istituto Tumori "Giovanni Paolo II" - Bari, Italy

Keywords: Multiple myeloma - Whole-body low-dose computed tomography - ^{18}F-FDG PET/CT - Multimodality imaging - Bone disease

Corresponding author:
Ferrari Cristina MD
Interdisciplinary Department of Medicine, Nuclear Medicine Unit; University of Bari Aldo Moro, Piazza Giulio Cesare 11 – 70124 Bari, Italy
Tel.: 0039 080 5595039
ferrari_cristina@inwind.it

Received:
9 October 2020
Accepted revised:
17 November 2020

Abstract

Objective: Whole body low dose computed tomography (WBLDCT) is the first-choice imaging modality to identify bone involvement in multiple myeloma (MM). Because the unenhanced LDCT co-registered to positron emission tomography (PET) (LDCT/PET) has similar technical characteristics to WBLDCT, we aimed to assess its reliability in the detection of bone disease, for employing fluorine-18-fluorodeoxyglucose (^{18}F-FDG) PET/CT as unique multimodality imaging method in MM patients. **Subjects and Methods:** Thirty three consecutive MM patients were prospectively enrolled and evaluated with WBLDCT to assess bone involvement. In addition, patients underwent ^{18}F-FDG PET/CT using a disease-tailored optimized LDCT protocol. To compare both methods, skeletal anatomical regions were identified and a per-region and per-patient analysis were performed using Cohen's k test. Low dose computed tomography/PET sensitivity, specificity and accuracy were also calculated. **Results:** The two imaging modalities resulted highly concordant considering both patient-based (k=0.841) and region-based analysis; some discrepancies were observed in dorsal spine (k=0.809) and thorax (k=0.756). Low dose computed tomography/PET sensitivity, specificity and accuracy were 89.4%, 98.3% and 93.5%, respectively. **Conclusion:** Low dose computed tomography co-registered PET has comparable performance to WBLDCT. If confirmed on a lager sample, these encouraging results suggest the possibility to use this multimodal hybrid imaging as the only method for MM evaluation, rather than both exams, providing both morphologic and metabolic information in one session with impact on patient compliance, health care spending and especially radiation exposure.

Hell J Nucl Med 2020; 23(3): 264-271 *Epub ahead of print: 14 December 2020* *Published online: 28 December 2020*

Introduction

Bone involvement is the most frequent feature of multiple myeloma (MM), occurring in approximately two-thirds of patients at diagnosis and in virtually all patients during the course of disease, impacting patient's quality of life as a major cause of morbidity and mortality [1].

Imaging plays a crucial role to assess bone involvement in all phases of MM disease: staging, restaging and evaluation of response to therapy. Conventional skeletal survey (CSS) has been considered for many years the gold standard to detect bone disease in these patients. However, the development and spread of novel, more advanced and sensitive cross-sectional imaging techniques, including computed tomography (CT), whole-body low-dose computed tomography (WBLDCT), magnetic resonance imaging (MRI) or fluorine-18-fluorodeoxyglucose positron emission tomography/CT (^{18}F-FDG PET/CT), allowed the start of a new era of both morphological and functional characterization of bone involvement [2].

Since 2014, according to the International Myeloma Working Group (IMWG), bone disease criteria are fulfilled in presence of at least one lytic focal bone lesion, revealed by CSS, WBLDCT, MRI or CT portion of ^{18}F-FDG PET/CT, crucial for starting anti-neoplastic treatment.

For this purpose, the employment of WBLDCT instead of CSS is strongly recommended in the workup of MM patients, due to its significantly higher sensitivity in detecting myeloma-related osteolytic lesions [3, 4]. Other advantages include that it is widely available, relatively cheap, simple to perform, and patient-friendly with a scanning time of less than one minute [5]. Whole-body low-dose computed tomography allows a whole-body skeletal system assessment with 3-fold lower radiation dose exposure compared to standard CT, preserving sensitivity, accuracy and adequate image quality [6, 7]. In fact,

although low dose reduces image quality (mainly owing to image noise), the study of the skeleton is not significantly impaired due to the intrinsic contrast between high-density mineralized bone and soft-tissue density of osteolytic lesions [8].

On the other hand, the advent of PET scanners has changed the approach to the assessment of MM patients from morphologic to a functional point of view. One of the most important advantages of ^{18}F-FDG PET is the ability to distinguish metabolically active myeloma (^{18}F-FDG-positive) from inactive disease; thus being the preferred method of therapy response evaluation [1, 9-11]. Changes in ^{18}F-FDG-avidity can provide an earlier evaluation of response to therapy and can predict outcome, particularly for patients who are eligible to receive autologous stem-cell transplantation, impacting patient's management, prognosis and definition of minimal residual disease [5, 12, 13]. Moreover, hybrid PET/CT scanners offer the possibility to achieve both metabolic and morphological information, making ^{18}F-FDG PET/CT the ideal multimodality imaging for the evaluation of MM patients: while ^{18}F-FDG PET detects areas with intense hypermetabolic activity, CT scan can visualize lytic lesions with a resolution limit of 0.5cm [14]. In fact, the unenhanced low-dose CT co-registered to PET (LDCT/PET) studies, performed for attenuation correction and lesion localization, presents technical characteristics comparable to WBLDCT.

However, although already Durie in 2006 argued that ^{18}F-FDG PET combined with CT scanning could have represented the ideal technology for MM patient evaluation, to the best of our knowledge, literature data still lack in providing a comparison between WBLDCT and LDCT/PET through prospective studies [15].

This study aimed to assess the reliability of unenhanced low-dose CT co-registered to PET compared to WBLDCT in the detection of bone disease for staging and restaging MM patients, in order to employ ^{18}F-FDG PET/CT as unique multimodality imaging method thanks to a combined radiologist-nuclear physician report.

Subjects and Methods

Study design

From September 2018 to January 2020, 33 consecutive patients (mean age: 67y, range: 53-82y) affected by MM were prospectively enrolled in this single-center study.

Inclusion criteria were: age >18 years, Eastern Cooperative Oncology Group (ECOG) performance status 0-2, need for diagnostic imaging to assess disease staging, restaging or relapse. A detailed staging was performed for each patient, including medical history, physical examination, laboratory parameters (including serum protein electrophoresis, 24-h urine collection, immunofixation in the serum and urine, b2-microglobulin, serum creatinine, serum calcium, and C-reactive protein), bone marrow aspirate or biopsy, if necessary. According to their regular workup, for the definition of bone involvement, patients underwent to WBLDCT, which was performed with different low dose CT protocols based on automatic modulation systems of radiation dose exposure.

In addition, enrolled patients underwent ^{18}F-FDG PET/CT at our Nuclear Medicine Department within 20 days (±5), with a dedicated disease-tailored low-dose CT protocol, as specified below.

The present prospective study was performed following the Declaration of Helsinki and approved by the local Ethics Committee (Prot. n. 828 CE, IRCCS Istituto Tumori "Giovanni Paolo II", Bari, Italy). All patients signed informed consent before study enrolment and were free to withdraw from the study at any time. No funding has been received for the study.

Baseline characteristics of the sample are reported in Table 1.

Table 1. *Patients' baseline characteristics.*

Patients' characteristics	**N= 33**	**% (100)**
Age at evaluation, years (mean, range)	65.4 (52-81)	
Male	15	45.4
Female	18	54.5
Asymptomatic MM	3	9
Symptomatic MM	29	88
Solitary plasmacytoma	1	3
Paraprotein	32	97
IgG (k/lambda)	19	59.4
IgA (k/lambda)	7	21.9
light chains (k/lambda)	6	18.8
Durie-Salmon stage at diagnosis	30	90.9
I	4	12.5
II A	1	3.1
II B	0	0
III A	26	81.3
III B	1	3.1
ISS stage at diagnosis	30	90.9
I	12	37.5
II	11	34,4
III	9	28.1
Lines of received chemotherapies	29	87.9
1	18	62
2	5	20.7
>/= 3	6	17.7

(continued)

Type of induction chemotherapy		
VTD	29	87.9
VCD	16	55.2
PAD	3	10.3
VMP	2	6.9
MPT	5	17.5
VD	1	3.4
others	1	3.4
autologous stem cell transplant	1	3.4
allogeneic stem cell transplant	9	31
	2	6.9

VTD: velcade (bortezomib), thalidomide, dexamethasone; VCD: velcade (bortezomib), cyclophosphamide, dexamethasone; PAD: modified bortezomib, adriamycin, dexamethasone; VMP: velcade (bortezomib), melphalan, prednisone; MPT: melphalan, prednisolone, thalidomide; VD, velcade (bortezomib), dexamethasone.

^{18}F-FDG PET/CT

According to EANM guidelines, ^{18}F-FDG PET/CT was performed after patient preparation that includes fasting for at least 6h, adequate hydration and capillary blood glucose of <160mg/mL. Images acquisition was obtained 50-60 minutes after the intravenous injection of 2.5MBq/kg of ^{18}F-FDG, by using a combined PET/CT scanner Discovery™ IQ (GE, Healthcare Technologies, Milwaukee, Wisconsin, USA) that integrates a 3D scanner PET with multidetector helical 16-slice CT scanner (light speed plus).

The CT data were used for attenuation correction of PET scanning, which was performed immediately after the acquisition of CT images. The PET acquisition was obtained in cranial-caudal direction, carried out from the skull to the femurs; PET was reconstructed with a matrix of 256x256, ordered subset expectation maximum iterative reconstruction algorithm (four iterations, 28 subsets), 8mm Gaussian filter, and 70cm field of view (FOV).

Low-dose CT protocol optimization

The unenhanced low dose CT performed as part of a PET/CT examination provides not only attenuation-correction but also diagnostic information that may be relevant to both PET interpretation and overall patient care. A variety of low dose CT protocols exists in the context of PET/CT scanning as well as numerous whole-body CT protocols are reported in the literature for MM patients.

In the present study, a low dose CT protocol co-registered to PET was developed following acquisition parameters specifically set for MM disease and chosen to optimize bone visualization, minimizing as much as possible radiation dose exposure according to ALARA principle and the European Directive legislation 97/43/EURATOM. In particular, the main difference compared with standard low dose CT acquisition parameters regarded the further reduction of mA range in the automated tube current modulation, ensuring good image quality both for PET and CT exams. Conversely, it was not possible to reduce the slice-thickness of 3.75 to assure the good attenuation correction for PET imaging, even if a very large set of images was obtained by modifying the reconstruction slice-thickness at 1.25mm on a dedicated workstation and evaluated in MPR and VR that decreased the likelihood of missing or misinterpreting findings.

Detailed LDCT parameters were reported in Table 2.

Table 2. *Computed tomography scan parameters of the optimization protocol LDCT/PET compared with standard CT acquisition parameters.*

Scan Parameters	Standard	Low dose
Tube voltage	120	120
Noise index	28.5	28.5
Pitch	0.938	0.938
Range	15-350mA	**15-70mA**
FOV/matrix	500mm/512	500mm/512
Detector configuration	16x1.25	16x1.25
Slice thickness	3.75	3.75
Reconstructed slice thickness	3.75	**1.25**

Patients were acquired in supine decubitus with arms positioned in front of the pelvis. This position was chosen to include arms in the FOV avoiding overlapping them with the spine for optimal image reading and interpretation. The FOV includes from the skull to the femurs (5-7 bed positions).

Images interpretation

Two independent readers experienced in skeletal imaging and CT (15 and 10 years of experience respectively) evaluated all preliminary WBLDCT and LDCT co-registered to PET studies in a non-sequential way; in the case of disagreement, they discussed until an agreement was reached. Readers were blinded to PET results and biochemical parameters.

To permit an easy and standardized comparison of both imaging techniques results, skeletal anatomical regions have been identified as follows: skull, spine (distinct in cervical, dorsal and lumbar), thorax (including ribs, sternum, scapula), pelvis, upper and lower limbs. Only osteolytic lesions with a diameter of 5mm or more were considered for the analysis.

Each exam was considered positive in the presence of at least one osteolytic bone lesion in at least one anatomical region. The number of anatomical regions involved in WBLDCT and LDCT/PET respectively was reported for each patient.

Then, the comparison between the two imaging techniques was performed on a per-region and a per-patient analysis respectively. To reduce bias, all exams were reviewed on the same reconstruction workstation (Intellispace Portal v 8.0; Philips Healthcare).

Statistical analysis

Cohen's k test was used to evaluate the concordance between LDCT/PET and WBLDCT on a per-region and a per-patient analysis. P value <0.05 was considered significant.

In addition, LDCT/PET sensitivity, specificity and accuracy were calculated by using WBLDCT as the gold standard.

Statistical analysis was carried out using IBM SPSS Statistics for Mac OS, version 20.0, 2012.

Results

A total of 264 anatomical regions were explored on LDCT/PET while 248 regions on WBLDCT in 33 MM patients. In 6/33 patients and 10/33 patients, upper limbs and lower limbs respectively were not included in the FOV of imaging scan of WBLDCT.

According to the patient-based analysis, 29/33 (88%) patients were considered positive at LDCT/PET while 30/33 (91%) at WBLDCT.

In particular, at least one osteolytic bone lesion was detected in a total of 120/264 (45%) and 132/248 (53%) anatomical regions on LDCT/PET and WBLDCT, respectively.

Detailed results of the imaging detection rate on the region-based analysis were described in Figure 1.

Considering the 248 comparable regions evaluated on both imaging methods, 118/248 (47.6%) regions were positive for both LDCT/PET and WBLDCT, 114/248 (46%) regions were negative for both exams, 14/248 (5.6%) were positive only on WBLDCT and 2/248 (0.8%) were positive only on LDCT/PET (false positive). Low-dose computed tomography/PET sensitivity, specificity and accuracy were 89.4%, 98.3% and 93.5% respectively.

The concordance between WBLDCT and LDCT/PET analysed by Cohen's k test is shown in Table 3.

The two imaging modalities resulted to be highly concordant, with no statistically significant differences between them, considering both the patient-based and region-based analysis.

In particular, according to the per-region analysis, the two methods were completely concordant in the cervical spine and lower limbs, while some discordant results were observed in dorsal spine, thorax, pelvis and upper limbs.

Low-dose computed tomography/PET detected one more positive anatomical region in 2/33 (6%) patients (1 in thorax and 1 upper limbs region); Whole-body low dose computed tomography detected one more positive anatomical region in 7/33 (21%) patients (3 in thorax, 1 in dorsal spine, 2 in pelvis and 1 in upper limbs region), two more positive anatomical regions in 2/33 (6%) patients (both in dorsal and lumbar spine region) and three more positive anatomical regions in 1/33 (3%) patient (skull, pelvis and upper limbs region).

No differences in the number of positive anatomical regions were found in the remnant 22/33 (67%) patients.

Representative images of concordant and/or discordant imaging results between WBLDCT and LDCT/PET are shown in Figures 2, 3 and 4.

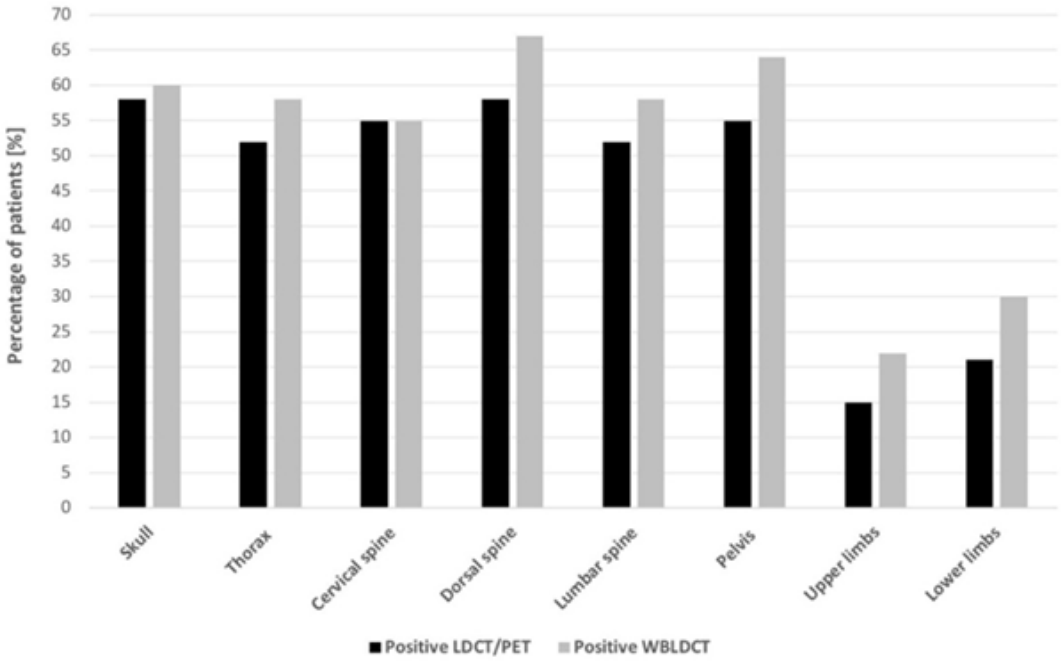

Figure 1. Imaging detection rate on the per-region results.

Table 3. *Concordance between WBLDCT and LDCT/PET in patient-based analysis and region-based analysis.*

	Positive Concordant	Negative Concordant	Discordant	Cohen's k Test	
				k	P value
Patient-based Analysis	29	3	1	0.841	<0.001
Region-based Analysis					
Skull	19	13	1	0.937	<0.001
Cervical spine	18	15	0	1.000	<0.001
Dorsal spine	19	11	3	0.809	<0.001
Lumbar spine	17	14	2	0.878	<0.001
Thorax (ribs, sternum, scapula)	16	13	4	0.756	<0.001
Pelvis	18	12	3	0.814	<0.001
Upper limbs	4	20	3	0.658	=0.001
Lower limbs	7	16	0	1.000	<0.001

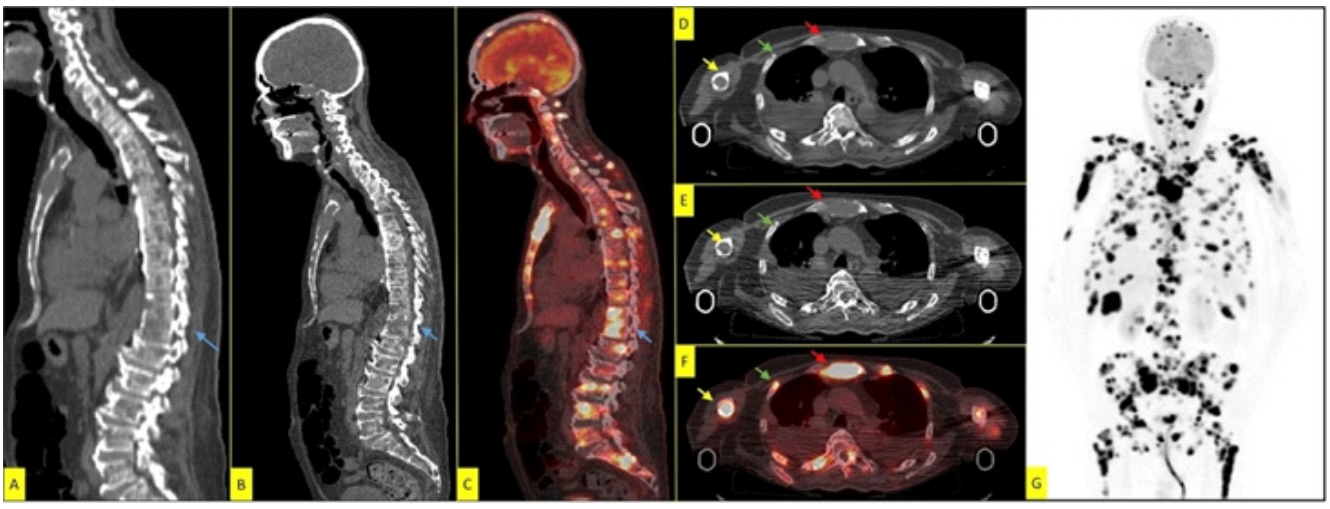

Figure 2. Whole-body low-dose computed tomography and ^{18}F-FDG PET/LDCT in staging a 66-year-old MM patient. Whole-body low-dose computed tomography (A, sagittal and D, axial) and LDCT co-registered to PET (B, sagittal and E, axial) images demonstrated comparable performance in detecting multiple osteolytic lesions in the sternum (red arrow), ribs (green arrow), vertebrae (blue arrow) and humerus (yellow arrow). In addition, PET imaging provided information about lesions metabolic activity in a single whole-body multimodal imaging examination (G, maximum intensity projection-MIP; C, sagittal and F, axial fused images).

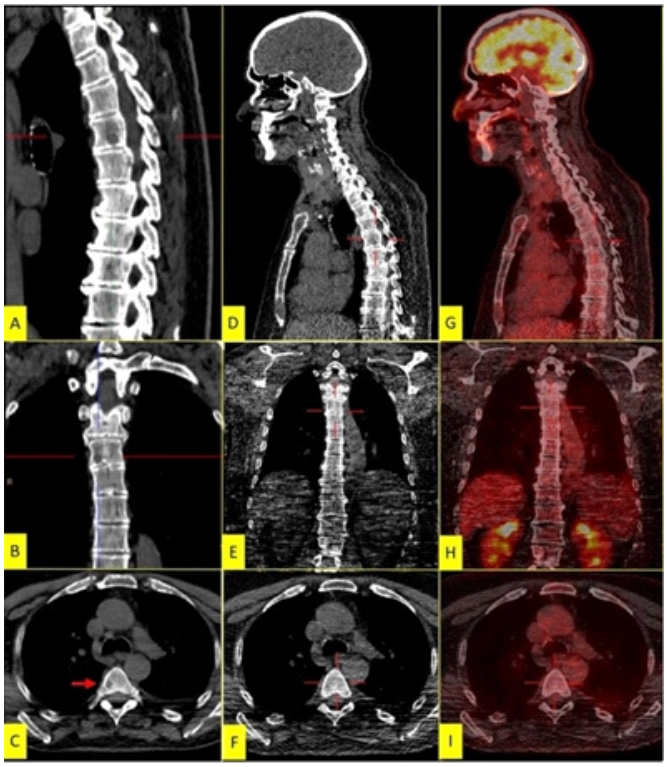

Figure 3. Whole-body low-dose computed tomography and ^{18}F-FDG PET/LDCT in staging a 73-year-old MM patient. Whole-body low-dose computed tomography (A, sagittal, B, coronal and C, axial) images showed an osteolytic lesion in D5, not seen on the LDCT co-registered to PET (D, sagittal, E, coronal and F, axial) images. Low-dose computed tomography/PET demonstrated lower performance than WBLDCT in evaluating osteolytic lesion of the dorsal spine , probably due to artifacts derived from uncorrected positioning of the upper limbs and high patient's BMI (31.8). Positron emission tomography (G, sagittal, H, coronal and I, axial) fused images documented the absence of metabolic activity in the lesion.

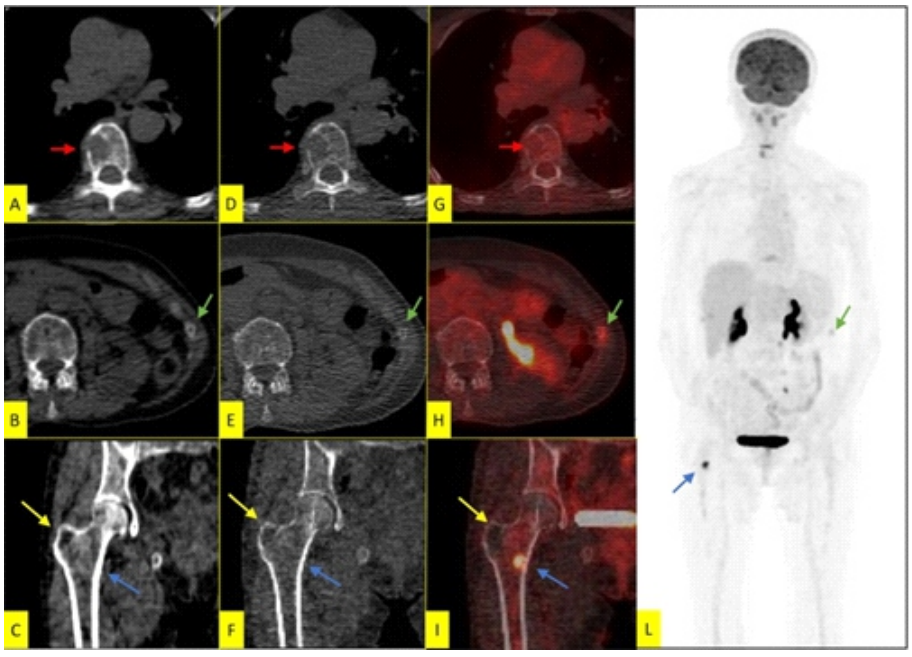

Figure 4. Whole-body low-dose computed tomography (A-C) and ^{18}F-FDG PET/LDCT (D-L) post-therapy evaluation in a 70-year-old MM patient. Whole-body low-dose computed tomography and LDCT co-registered to PET agreed in detecting osteolytic lesions in D8 (A, D - red arrow) and in the greater trochanter of the right femur (C, F - yellow arrow), while the osteolytic lesion of the left rib was detected exclusively on WBLDCT images (B, E - green arrow). In addition, PET imaging documents inactive lesions in D8 (G - red arrow) and in the greater trochanter of the right femur (I - yellow arrow), with the appearance of active ones in the left rib (H - green arrow) and of the lesser trochanter of the right femur (I - blue arrow). This latter lesion does not show morphological alterations both on WBLDCT and LDCT/PET images (A-F) for early medullary localization. Whole-body multimodal imaging allowed to highlight the simultaneous presence of metabolically active and inactive lesions.

Discussion

Bone disease occurs in 80%-90% of MM patients and represents the main cause of skeletal-related events associated with increased morbidity and mortality [5].

Even if the confirmed diagnosis of bone involvement is histologic, imaging plays a crucial role to assess the degree of skeletal involvement and to guide the therapeutic decision-making process, according to the International Myeloma Working Group (IMWG) criteria for monoclonal gammopathies and multiple myeloma [5, 12, 16, 17].

To date, WBLDCT is the first-choice cross-sectional imaging recommended for MM bone disease evaluation by IMWG and ESMO guidelines [13, 17]. Several varying protocols for whole-body CT have been reported; for example Hemke et al. (2020) described six different multi-detector CT scanners and related WBLDCT protocols in the same study, emphasizing their impact on clinical practice and radiation exposure dose in MM work-up [18]. Even if Moulopoulos et al. (2018) tried to provide practical recommendations for the acquisition, interpretation and reporting of WBLDCT studies in MM patients, a published consensus on the adequate technical requirement and standardization guidelines is still lacking [5].

On the other hand, ^{18}F-FDG PET/CT is a multimodal whole-body exam that combines functional imaging with morphological evaluation in one session and in a reasonable timeframe, providing integrated information of fundamental importance to guide clinicians in different phases of MM disease [12]. Whilst functional portion of PET/CT exam allows to distinguish between metabolically active and inactive disease, useful to monitor and evaluate therapy efficacy on myeloma-cell metabolism [10, 19], the increased ^{18}F-FDG uptake alone is not adequate for diagnosis of MM [3]. As clarified by the IMWG, the evidence of underlying osteolytic bone destruction on the CT portion of PET/CT fulfills the criteria for bone disease [3], making the LDCT co-registered to PET the additional morphological method able to assess MM-related bone features.

Actually, WBLDCT and LDCT co-registered to PET have similar technical characteristics. However, to the best of our knowledge, this is the first study that prospectively compared the performance of LDCT/PET and WBLDCT in MM patients. Few studies considered the diagnostic performance of CT co-registered to PET for detecting bone destruction in MM patients but comparing it to standard skeletal survey or MRI, underlying the importance of using more specific imaging techniques to avoid inaccurate diagnosis [20-22].

As for the WBLDCT, also the LDCT co-registered to PET lacks standardized protocols and various attempts to optimize the acquisition parameters have been suggested to maximize the benefit/risk ratio and ensure both an adequate assessment of target organs and compliance with ALARA principle of radiological protection [16, 23, 24].

In the present study, based also on the protocol reported by Cretti et al. (2016) [16], our efforts were focused on developing a specific, reproducible and standardized protocol tailored for MM patients characterized by the lowest possible radiation exposure dose while preserving high imaging quality of the bone, considering the intrinsic contrast between high-density mineralized bone and soft-tissue density of osteolytic lesions. In particular, the main difference compared with standard CT co-registered to PET acquisition parameters regarded the reduction of mA range in the automated tube current modulation (up to 70mA), without compromising the attenuation correction and image quality for PET exam [6, 8].

In this way, we achieved an average dose length product (DLP) of LDCT/PET performed in patients enrolled in our study of 250mGy/cm, that represented a significant reduction in radiation exposure dose compared to 400mGy/cm of the standard examination [25]. In this setting, patients positioning has a crucial role, taking into account that if arms are placed alongside the body, a 30% greater radiation dose is required to compensate for the attenuation caused by the arms [6]. In our study, patients were acquired in supine decubitus with arms positioned in front of the pelvis, to include them in the FOV without superimposing on the dorsal and lumbar spine and mitigating certain artifacts, including beam hardening and ring artifacts. Although this patient positioning allowed us to better evaluate column as site often affected, it led to overlap the arms on the ribs, notoriously a challenge due to their small size, making the thorax the anatomical region with major discrepancy between LDCT/PET and WBLDCT in our study [5].

The high body mass index (BMI) represented another factor that compromised diagnostic performance of LDCT/PET, making difficult the detection of lytic bone lesions in some anatomical regions (dorsal and lumbar spine and pelvis), despite the significant reduction of absorbed dose. A future perspective could be the possibility to further adapt the protocol in this setting of patients.

Despite these limitations, our data demonstrated that LDCT co-registered to PET, even if performed according to a specific protocol tailored for MM patients with a significant radiation exposure dose reduction, has comparable performance to WBLDCT.

Further studies are needed to confirm these encouraging results on a larger sample and to develop standardized low-dose CT protocol and image interpretation criteria.

In conclusion, currently, WBLDCT is the first-choice imaging modality for the assessment of bone disease in MM patients. However, in our study LDCT co-registered to PET demonstrated comparable performance with high sensitivity, specificity and accuracy. These encouraging results suggest the possibility that in the next future ^{18}F-FDG PET/CT could be performed, if available, as unique multimodality imaging method, rather than both exams, during MM patients work-up, with the capability to provide both morphologic and additional metabolic information in one session. A thorough report to include the PET and the CT findings is crucial, especially in MM, as both information could impact patient management, prognosis and finally heath care spending.

The authors declare that they have no conflicts of interest.

Bibliography

1. Rubini G, Niccoli-Asabella A, Ferrari C et al. Myeloma bone and extra-medullary disease: Role of PET/CT and other whole-body imaging techniques. *Crit Rev Oncol Hematol* 2016; 101: 169-83.
2. Barwick T, Bretsztajn L, Wallitt K et al. Imaging in myeloma with focus on advanced imaging techniques. *B. J Radiol* 2019; 92(1095): 20180768.
3. Rajkumar SV, Dimopoulos MA, Palumbo A et al. International Myeloma Working Group updated criteria for the diagnosis of multiple myeloma. *Lancet Oncol* 2014; 15: e538–48.
4. Hillengass J, Moulopoulos LA, Delorme S et al. Whole-body computed tomography versus conventional skeletal survey in patients with multiple myeloma: A study of the International Myeloma Working Group. *Blood Cancer J* 2017; 7(8):e599.
5. Moulopoulos LA, Koutoulidis V, Hillengass J, et al. Recommendations for acquisition, interpretation and reporting of whole body low dose CT in patients with multiple myeloma and other plasma cell disorders: a report of the IMWG Bone Working Group. *Blood Cancer J* 2018; 8(10): 95.
6. Lambert L, Ourednicek P, Meckova Z et al. Whole-body low-dose computed tomography in multiple myeloma staging: Superior diagnostic performance in the detection of bone lesions, vertebral compression fractures, rib fractures and extraskeletal findings compared to radiography with similar radiation exposure. *Oncol Lett* 2017; 13(4): 2490-4.
7. Pianko MJ, Terpos E, Roodman GD et al. Whole-body low-dose computed tomography and advanced imaging techniques for multiple myeloma bone disease. *Clin Cancer Res* 2014; 20(23): 5888-97.
8. Chantry A, Kazmi M, Barrington S et al. Guidelines for the use of imaging in the management of patients with myeloma. *Br J Haematol* 2017; 178(3): 380-93.
9. Lütje S, de Rooy JW, Croockewit S et al. Role of radiography, MRI and FDG-PET/CT in diagnosing, staging and therapeutical evaluation of patients with multiple myeloma. *Ann Hematol* 2009; 88(12): 1161-8.
10. Dammacco F, Rubini G, Ferrari C et al. ^{18}F-FDG PET/CT: a review of diagnostic and prognostic features in multiple myeloma and related disorders. *Clin Exp Med* 2014; 15(1): 1-18.
11. Kumar S, Paiva B, Anderson KC et al. International Myeloma Working Group consensus criteria for response and minimal residual disease assessment in multiple myeloma. *Lancet Oncol* 2016; 17(8): e328-46.
12. Cavo M, Terpos E, Nanni C et al. Role of ^{18}F-FDG PET/CT in the diagnosis and management of multiple myeloma and other plasma cell disorders: a consensus statement by the International Myeloma Working Group. *Lancet Oncol* 2017; 18(4): e206-17.
13. Hillengass J, Usmani S, Rajkumar SV et al. International myeloma working group consensus recommendations on imaging in monoclonal plasma cell disorders. *Lancet Oncol* 2019; 20(6): e302-12.
14. Zamagni E, Cavo M. The role of imaging techniques in the management of multiple myeloma. *Br J Haematol* 2012; 159(5): 499-513.
15. Durie BG. The role of anatomic and functional staging in myeloma: Description of Durie/Salmon plus staging system. *Eur J Cancer* 2006; 42(11): 1539-43.
16. Cretti F, Perugini G. Patient dose evaluation for the whole-body low-dose multidetector CT (WBLDMDCT) skeleton study in multiple myeloma (MM). *Radiol Medica* 2016; 121(2): 93-105.
17. Zamagni E, Tacchetti P, Cavo M. Imaging in multiple myeloma: How? When? *Blood* 2019; 133(7): 644-51.
18. Hemke R, Yang K, Husseini J et al. Organ dose and total effective dose of whole-body CT in multiple myeloma patients. *Skeletal Radiol* 2020; 49(4): 549-54.
19. Ferrari C, Niccoli Asabella A, Merenda N et al. Pediatric Hodgkin Lymphoma. *Med. (United States)* 2017; 96(5): e5973.
20. Zamagni E, Nanni C, Patriarca F et al. A prospective comparison of ^{18}F-fluorodeoxyglucose positron emission tomography-computed tomography, magnetic resonance imaging and whole-body planar radiographs in the assessment of bone disease in newly diagnosed multiple myeloma. *Haematologica* 2007; 92(1): 50-5.
21. Rasch S, Lund T, Asmussen JT et al. Multiple myeloma associated bone disease. *Cancers (Basel)* 2020; 12(8): 2113.
22. Hill E, Mena E, Morrison C et al. Diagnostic performance of ^{18}F-FDG-PET/CT compared to standard skeletal survey for detecting bone destruction in smouldering multiple myeloma: time to move forward. *Br J Haematol* 2020; doi:10.1111/bjh.17088.
23. Quinn B, Dauer Z, Pandit-Taskar N et al. Radiation dosimetry of ^{18}F-FDG PET/CT: Incorporating exam-specific parameters in dose estimates. *BMC Med Imaging* 2016; 16(1): 41.
24. ACR-SPR Acr-Spr Practice Parameter for Performing FDG-PET/CT in Oncology Preamble. 2016; 1076: 1-17.
25. Huda W, Mettler FA. Volume CT Dose Index and Dose-Length Product Displayed. *Radiology* 2011; 258(1):236-42.